

Ab Initio Study of Structural, Electronic and Optical Properties of Full-Heusler Compound Co_2MnZ ($Z=\text{Si, Ge}$) Using Wien2k Code

J. Bhavani^{1*}, Bhavhani K¹¹Department of Physics, Ethiraj College for Women, Chennai-600 008, (T. N.), IndiaDOI: [10.36347/sjpm.2021.v08i08.004](https://doi.org/10.36347/sjpm.2021.v08i08.004)

| Received: 17.09.2021 | Accepted: 26.10.2021 | Published: 30.10.2021

*Corresponding author: J. Bhavani

Abstract**Original Research Article**

The structural, electronic and optical properties of the full Heusler compounds Co_2MnZ ($Z= \text{Si, Ge}$) have been studied using the Wien2k application. Half metallic ferromagnetism has been predicted in these compounds using the first principle calculations. The Full Potential Linearized Augmented Plane Wave (FP-LAPW) method along with local orbitals have been incorporated to solve the Hamiltonian of the system and hence to study the properties. The exchange-correlation potential is determined using PBE-GGA (Perdew, Becke, and Enzerhof-Generalized Gradient Approximation) potential. Among various full Heusler compounds, these compounds have been concentrated because of its enormous applications in the field of spintronics and magneto electronics. The property of half metallicity makes these compounds unique and noticeable from other compounds of the same class. The results have been compared with the available theoretical data the results obtained from this work were in good agreement with the compared theoretical values.

Keywords: Structural properties, Electronic properties, optical properties, half metallic ferromagnets, first principle calculations, FP-LAPW, PBE-GGA, spintronics, magneto electronics.

Copyright © 2021 The Author(s): This is an open-access article distributed under the terms of the Creative Commons Attribution 4.0 International License (CC BY-NC 4.0) which permits unrestricted use, distribution, and reproduction in any medium for non-commercial use provided the original author and source are credited.

1. INTRODUCTION

Heusler alloys are a fascinating class of materials with unique properties like half-metallic ferromagnetism, shape memory alloys, thermoelectric properties, and superconductivity. This uniqueness makes these alloys as promising candidates in the field of spintronics and magneto electronics. Heusler alloys are classed into four types namely full Heusler alloys, semi Heusler alloys, Quaternary Heusler alloys and inverse Heusler alloys having the stoichiometric composition of X_2YZ , XYZ , $\text{XX}'\text{YZ}$ and X_2YZ (with XXYZ position) respectively [1]. This work emphasizes the full Heusler alloy compounds, Co_2MnSi and Co_2MnGe . Co-based Heusler alloys are of great curiosity because of its prominent half-metallic nature when spin-polarized around the Fermi level that is these compounds show metallic nature in the majority spin projection and semiconducting nature in the minority spin projection. This feature has fascinating applications like spin injection devices, spin filters, tunnel junctions, Tunnel Magneto Resistance (TMR) and Giant Magneto Resistance (GMR).

In this work the structural, electronic and optical properties of the full Heusler alloys are analyzed using the first principle calculations in Wien2k code.

2. COMPUTATIONAL METHODS

Wien2k is one of the fastest and reliable simulation codes among computational methods which is based on the Density Functional Theory (DFT). This application is coded using FORTAN90 program. It was developed in the year 2000(2k) from Vienna hence the name Wien2k. The Fortan90 program helps in performing quantum mechanical calculations on periodic solids. The main developers of this application are P. Blaha, K. Schwarz, G. Madsen, D. Kvasnicka, J. Luitz [1]. In this study the first principle calculations are studied within the frame work of DFT using the all-electron Full Potential Linearized Augmented Plane Wave method along with local orbital (FP-LAPW+lo). The exchange correlation potential is given by PBE-GGA (Perdew, Becke, and Enzerhof-Generalized Gradient Approximation) method [2]. In FP-LAPW method the crystal space is divided using muffin tin spheres of suitable radius known as muffin tin radius

(Rmt). These spheres are non-overlapping and the space between the spheres are considered as interstitial regions. Inside the muffin tin sphere, the basis is expanded into spherical harmonic functions and in the interstitial region it is expanded into Fourier series. The Rmt values for the compound Co_2MnSi are given as 2.280 for Co and Mn and for Si 1.880. Similarly, for the compound Co_2MnGe , 2.320 for Co and Mn whereas for Ge it is considered as 2.260. To initialize the self-consistent field (SCF) it is important to mention the number of k points which is approximately given as 1000k points for both Co_2MnSi and Co_2MnGe .

3. RESULTS AND DISCUSSION

3.1 Structural Properties

In this work, the structural properties of full Heusler compounds Co_2MnZ (Z=Si, Ge) are studied.

Both the compounds crystallize in L21 structure which owns the space group $\text{Fm}\bar{3}\text{m}$ (no 225) [3]. The L21 structure is composed of four interpenetrating face centered cubic (fcc) lattices. The positions are described using Wyckoff coordinates as A (1/4,1/4,1/4), B (1/2,1/2,1/2), C (3/4,3/4,3/4), D (0,0,0). The full Heusler compounds taken into consideration have the crystal configuration XYXZ where X (Co_2 -Cobalt) atom occupies the positions A and C given by 8c (1/4,1/4,1/4) and 8c (3/4,3/4,3/4). The Y (Mn-Manganese) atom occupies the position 4a (1/2,1/2,1/2) and finally the Z (Si/Ge-Silicon or Germanium) atom occupies 4b (0,0,0). The crystal structure of the compounds (Figure 1 and Figure 2) are determined using the application called Xcrysden which is an inbuilt program in Wien2k.

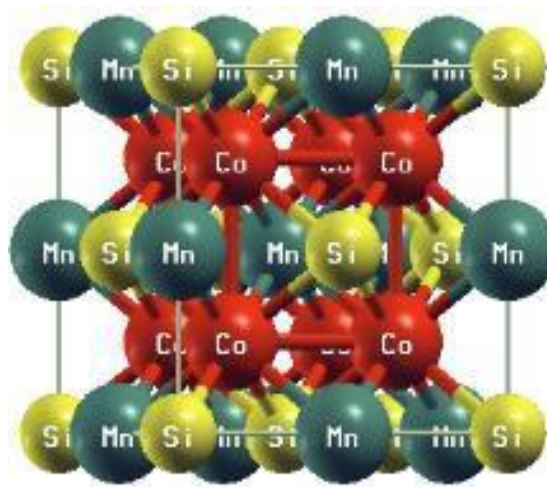


Figure 1: Co_2MnSi crystal structure

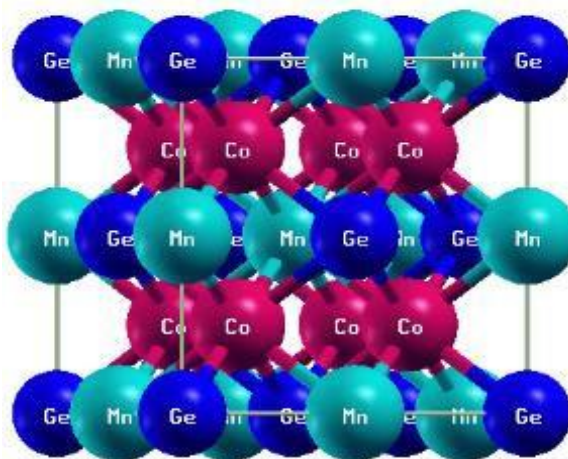


Figure 2: Co_2MnGe crystal structure

The compounds Co_2MnZ is a cubic crystal with the lattice parameters $a=b=c$ and the interplanar angles $\alpha=\beta=\gamma=90^\circ$. The lattice parameters of the compounds before and after optimization are given in Table 1. The data is compared with the available theoretical values. The lattice constants of the experimental data and optimized values are compared and it is found that the observed value of Co_2MnSi is less than the value recorded in the experimental and theoretical methods whereas for Co_2MnGe the observed value is higher than the experimental and theoretical values.

Table 1: Lattice parameters compared with the experimental and theoretical data

Compound	Data	Lattice parameter Å	Interplanar angles
Co ₂ MnSi	This work before optimization	5.606 ⁽³⁾	$\alpha=\beta=\gamma=90^\circ$
	This work after optimization	5.606	
	Theoretical	5.634 ⁽⁴⁾ ,5.523 ⁽⁴⁾	
Co ₂ MnGe	This work before optimization	5.711	
	This work after optimization	5.895	
	Theoretical	5.734 ⁽⁴⁾ ,5.753 ⁽⁴⁾	

In order to determine the ground state properties, such as equilibrium lattice volume, bulk modulus, pressure derivative of bulk modulus, the total energy variation with respect to volume etc. is fitted to

the Birch-Murnaghan's equation of state (EOS) [2]. The optimization curve is given in Figure 3 and Figure 4 for Co₂MnSi and Co₂MnGe compounds respectively.

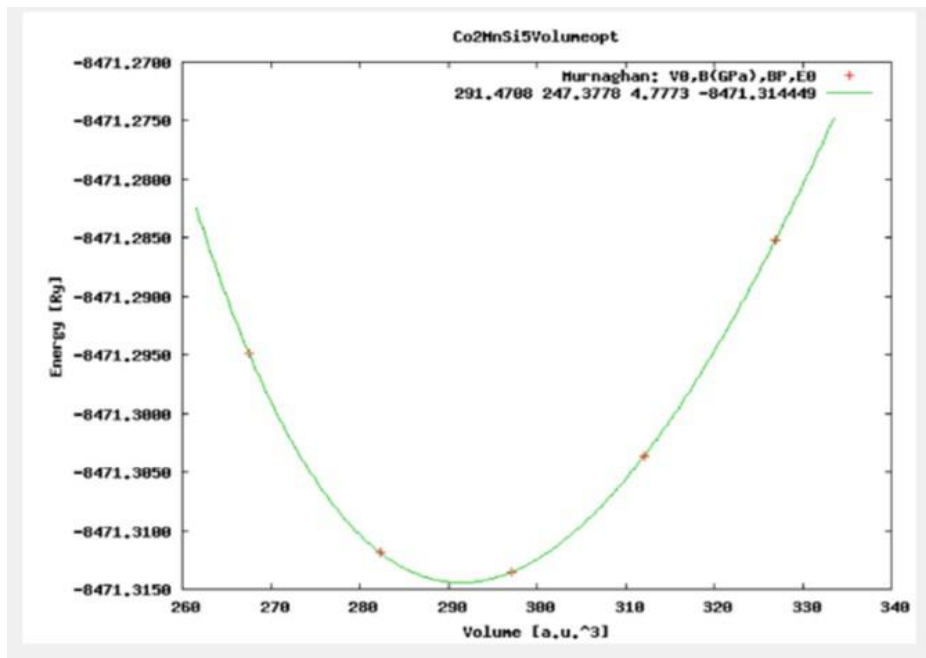


Figure 3: Volume optimization of Co₂MnSi

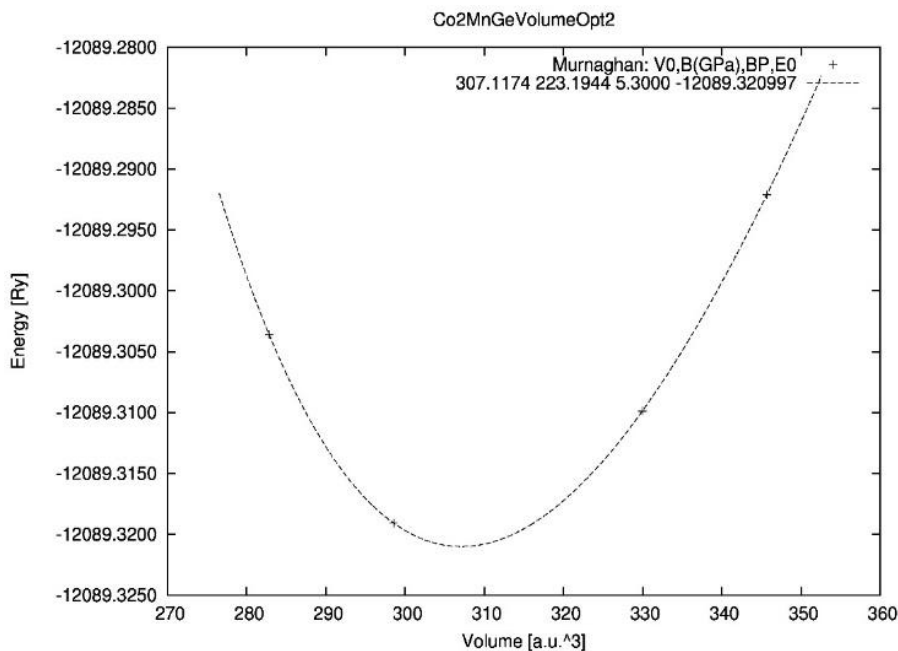


Figure 4: Volume optimization of Co₂MnGe

The data obtained from the volume optimization like lattice constant, equilibrium lattice volume bulk modulus is given in Table 2. These data are compared with the available theoretical values. It is observed from Table 2 that the lattice constant increases with the atomic number of the Z atom when Si is replaced with Ge. Correspondingly the lattice constant of Ge is greater than Si (Table 2) thus proving that lattice constant is directly proportional to the atomic radii of the atom. As the lattice constant increases from Si to Ge the equilibrium lattice value also increases which in turn decreases the bulk modulus [2, 3]. The bulk modulus value determines the rigidity of the crystal. The bulk modulus of Co₂MnSi is larger than Co₂MnGe thus making Co₂MnSi more rigid than

Co₂MnGe. The bond length of the compounds is observed and it is found that the bond order is inversely proportional to the bond length that is as the bond length decreases the bond order increases. When a bond is strong the bond length is shorter and the bond order is larger thus making the structure more stable whereas when the bond energy is considered it is high for the system having small bond length [5]. From Table 3 it is observed that the bond length of Co₂MnSi is smaller when compared to Co₂MnGe. The Δ B.L (Difference in bond length) for Co₂MnSi is given as 0.0783 and that of Co₂MnGe is given as 0.0799. Shorter the bond length more stable the system is hence here Co₂MnSi is more stable than Co₂MnGe because Co₂MnSi is having relatively smaller bond length than Co₂MnGe.

Table 2: Lattice constant, bulk modulus, pressure derivative of bulk modulus and total energy values for the compounds Co₂MnSi and Co₂MnGe

Compounds	Lattice constant [Å]	Equilibrium Lattice volume [a. u ³]	Bulk modulus [Gpa]	Pressure derivative of bulk modulus [Gpa]	Total Energy [Ry]
Co₂MnSi:					
This work	5.606	291.4788	247.3778	4.7773	-8471.31449
Theoretical		-	226 ⁽⁴⁾	4.674 ⁽⁴⁾	8471.432947 ⁽³⁾
Co₂MnGe:					
This work	5.895	307.1174	223.1944	5.3000	-12089.320997
Theoretical		308.3144 ⁽⁵⁾	216.62 ⁽⁵⁾	4.54 ⁽⁴⁾	-12089.325 ⁽⁵⁾

Table 3: Bond length (B.L) between XY, YX, XZ atoms in the Heusler compounds Co₂MnSi and Co₂MnGe

Compound	Bond length of Co-Mn (Å)	Bond Length of Mn-Co (Å)	Bond length of Co-Z(Si/Ge) (Å)
Co₂MnSi:			
B.L before optimization:	2.4275	2.4275	2.4275
B.L after optimization:	2.5058	2.5058	2.5058
ΔB. L (Difference in bond length)	0.0783	0.0783	0.0783
Co₂MnGe:			
B.L before optimization:	2.4729	2.4729	2.4729
B.L after optimization:	2.5528	2.5528	2.5528
ΔB. L (Difference in bond length)	0.0799	0.0799	0.0799

3.2 Electronic Properties

Electronic charge distribution, Density of States (DOS) and the band structure of the compounds are analyzed in the electronic properties. The electronic charge distribution helps to determine the nature of the chemical bond between the atoms. The 3-dimensional plot (Figure 5 and Figure 6) and contour plot (Figure 7) are studied using wien2k application. The 3D plot

determines the electron accumulation around the atom whereas the contour plot gives the chemical bonding nature. Covalent bonding nature is seen in both the spins for the compounds [6]. This result is established due to the presence of isolines in the contour plot given in Figure 7. When the majority spin and minority spins are compared from Figure 7, the covalency is more in the minority spin than the majority spin.

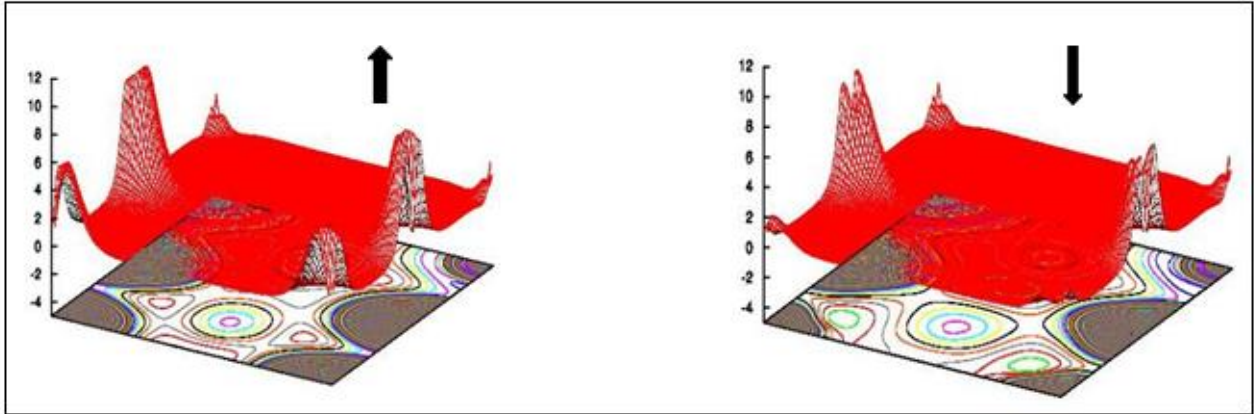


Figure 5: Electronic charge Distribution Co_2MnSi in (100) plane electron density 3d plot for majority (up arrow) and minority spin (down)

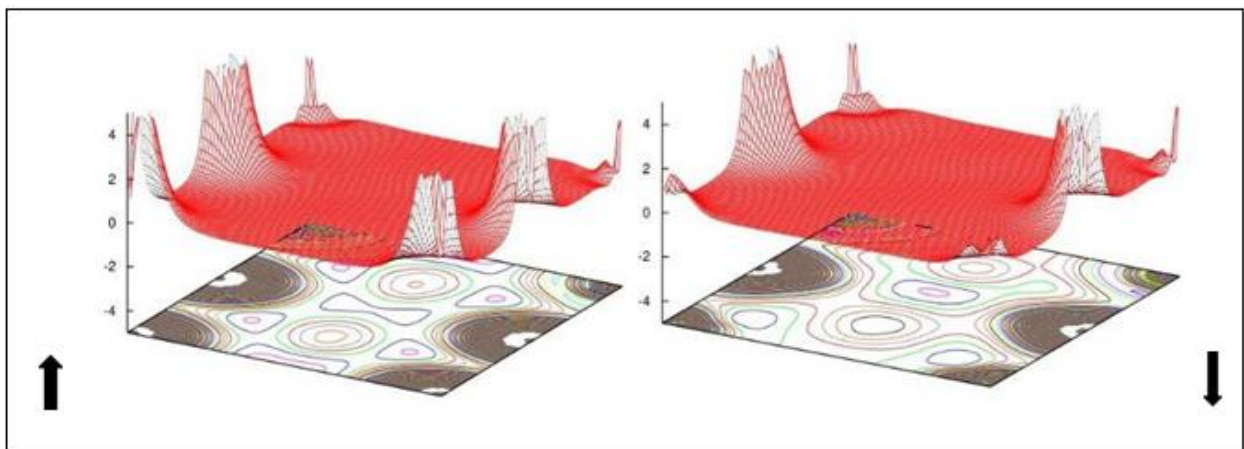


Figure 6: Electronic charge Distribution Co_2MnGe in (100) plane electron density 3d plot for majority (up arrow) and minority spin (down arrow)

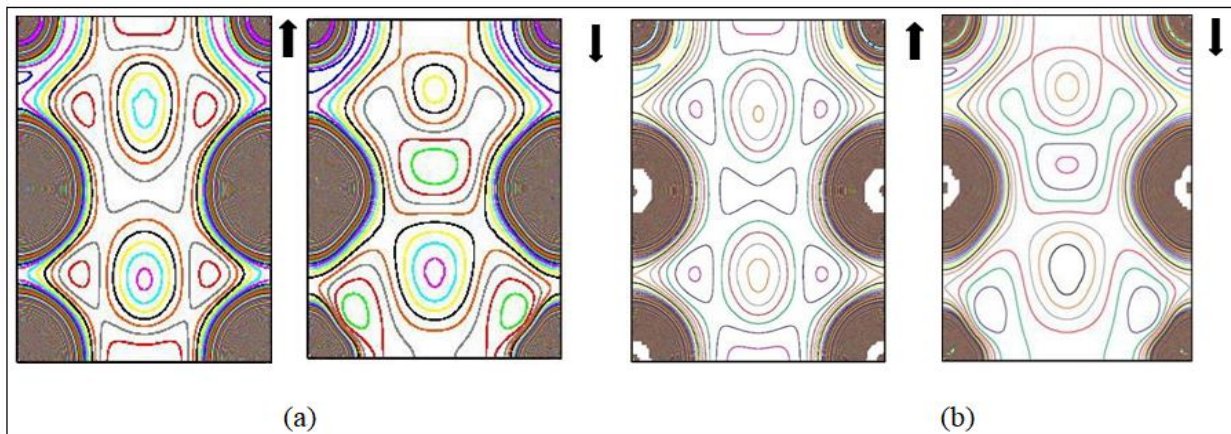


Figure 7: Electronic charge Distribution Co_2MnSi (a) and Co_2MnGe (b) in (100) plane electron density contour plot for majority (up arrow) and minority spin (down arrow)

The Density of States (DOS) signifies the different atomic orbital contribution of the elements to the band structure of the compounds. The total DOS (TDOS) and partial DOS (PDOS) are given in Figure 8 and Figure 9 respectively for the compound Co_2MnSi . Similarly, for the compound Co_2MnGe the TDOS and PDOS are given in Figure 10 and Figure 11

respectively. Considering the compound Co_2MnSi , when the TDOS (Figure 8) and PDOS (Figure 9) are compared it is clear that the electronic states to the lower side of the fermi energy level that is the valence band, is mainly contributed by the 3d electrons of the Mn atoms and 3d electrons of the Co atom. While comparing the TDOS and PDOS it is evident that the

majority contribution is given by 3d electrons of Mn atoms and from Fig.20 (e) it is clear that sp orbitals of the Si atom contributes the least to the TDOS of Co₂MnSi [5].The maximum peak in the majority spin of TDOS is found at approximately -1.8eV and this peak is mainly contributed by the 3d electrons of the Mn atoms. It is important to observe that there is negligible contribution of Co and Mn atoms in the spin up channel above the fermi energy level [7]. The contribution of s electron in the PDOS of Co and Mn is negligible. The majority spin DOS is strongly metallic and minority spin DOS shows semiconducting nature due to the gap around the fermi level [8].

In the spin down DOS the curves exhibit two peaks above the fermi level which are due to both Mn and Co 3d hybridization. It is also eminent that the minority d states of Mn are generally shifted to higher energies compared to the d orbitals of Co due to strong exchange splitting at the Mn atoms [9].It has been observed from the Figure 10 that majority spin shows

metallic nature and minority spin shows semiconducting nature thus turning out to be half metallic like Co₂MnSi. On examining TDOS and the atomic projected DOS for majority spin shown in Figure 10 and Figure 11 respectively it is evident that in majority spin the chief contribution is due to Mn 3d electrons and the second important contribution is from Co 3d electrons whereas least contribution is given by Ge atom to the TDOS. In the minority spin DOS shown in Figure 11 in the energy region below EF that is in region approximately around -2eV to -1eV there is a sharp peak which is mainly due to the 3d electrons of the Co atom thus making it [10] contribute more to the TDOS in the minority spin. The peak in the region -4eV to -2eV is due to Mn and Co 3d electrons. The fermi level is set at 0eV represented by dotted lines. The EF lies closer to the valence band when compared with that of the conduction band peak [4]. The energy gap in the minority spin is due to the eg-t2g hybridization of Co and Mn d orbitals which is similar to the concept explained in Co₂MnSi DOS [10].

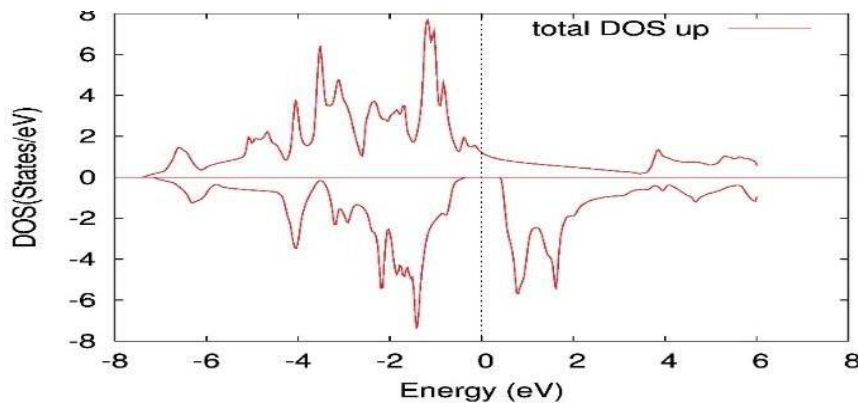


Figure 8: TDOS of Co₂MnSi

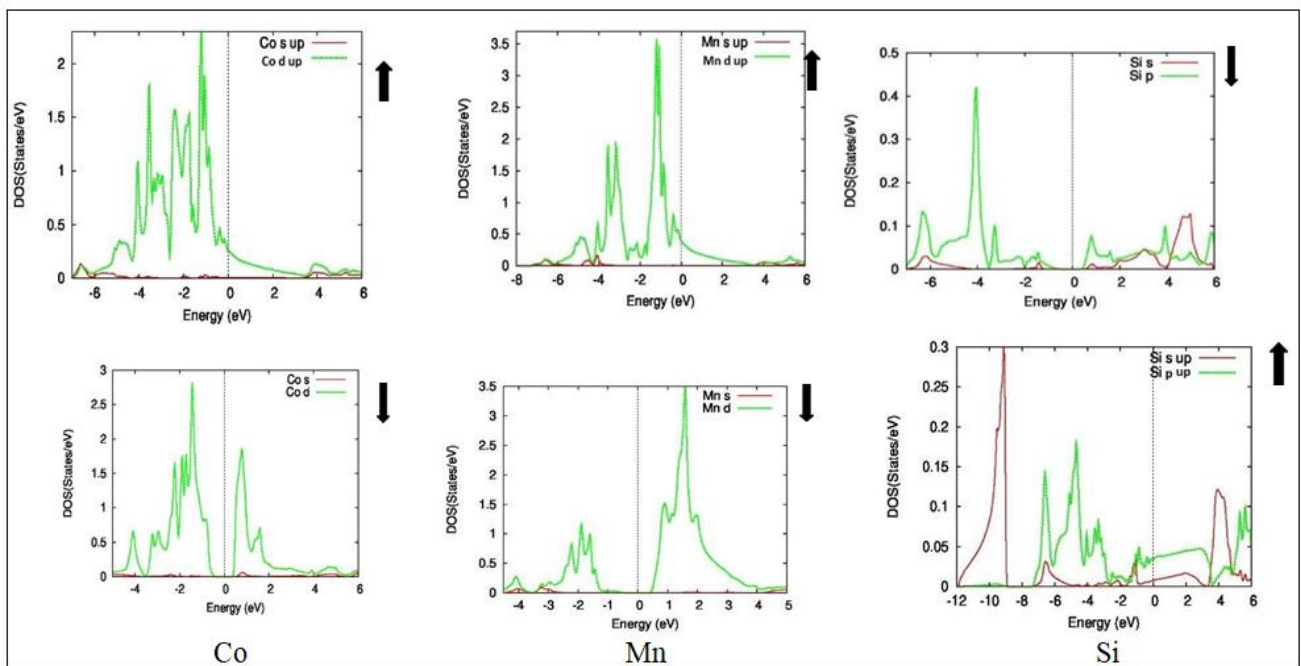


Figure 9: PDOS of Co₂MnSi for both majority (up arrow) and minority spin (down arrow)

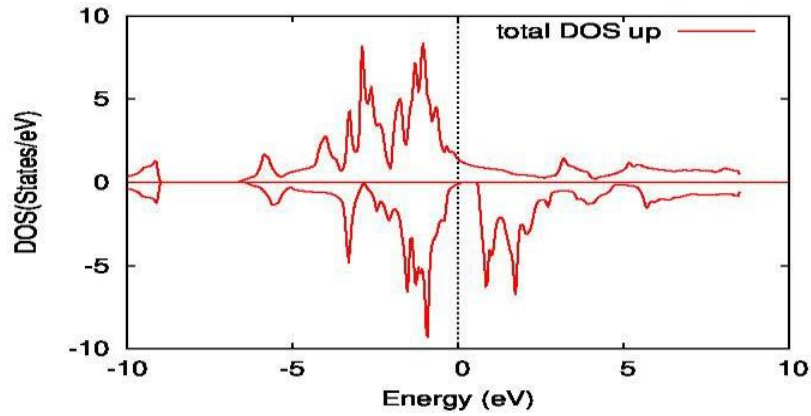


Figure 10: TDOS of Co_2MnGe

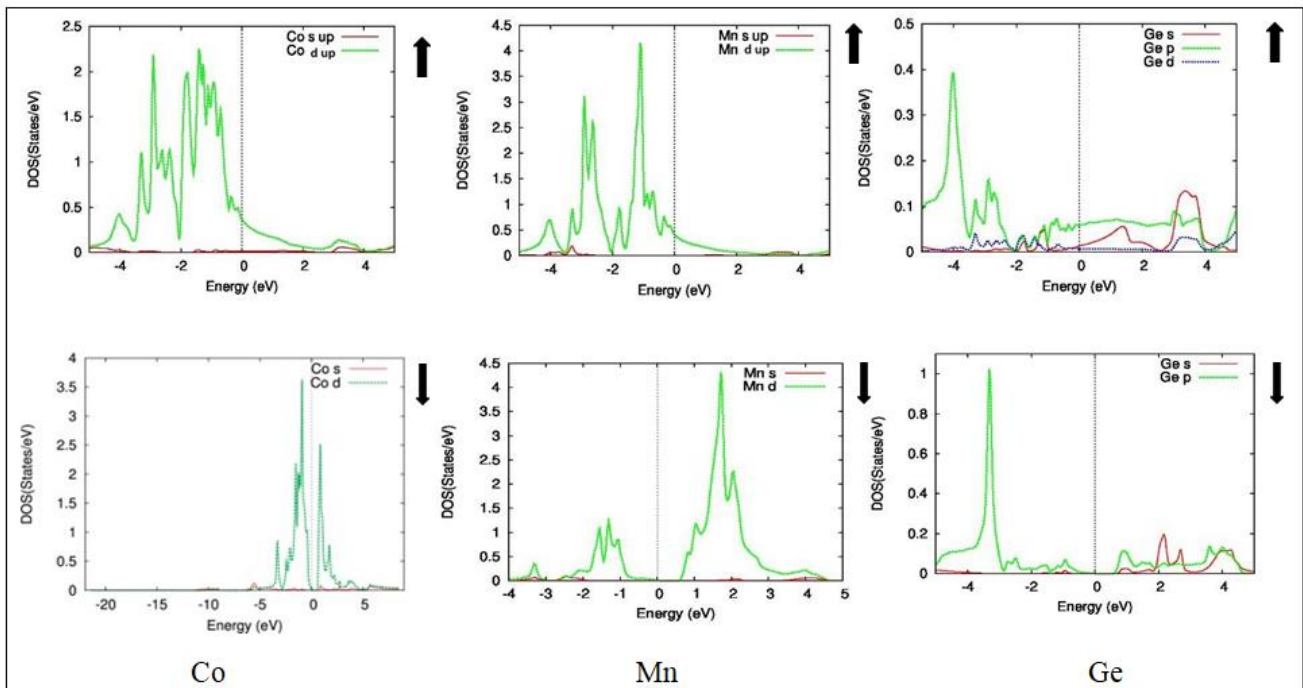


Figure 11: PDOS of Co_2MnGe for both majority (up arrow) and minority spin (down arrow)

Band structure plays an important role in the electronic properties of a compound. Using PBE GGA approximation the band structure for both up and down spins for the compounds Co_2MnSi (Figure 12) and Co_2MnGe (Figure 13) are calculated. The Fermi level is set at 0eV. The band structure for both the compounds show half metallicity. That is in majority spin the compounds show metallic nature with overlapping energy levels and in the minority spin the compounds show semiconducting nature with a forbidden energy gap at the Fermi level [3]. Thus, the compounds show a true half metallicity with 100% spin polarisation at the Fermi level. From Figures 12 and 13 the valence band maximum (VBM) lies in the Γ space and the conduction band minimum (CBM) lies in the X space thus depicting the indirect bandgap [10]. In the minority spin band structure for both the compounds it can be

observed that the valence band maximum for Co_2MnGe is comparatively closer to the Fermi energy level than in Co_2MnSi . This shows that the upper valence bands shift towards the Fermi level E_F when the atomic number increases. The PDOS and the band structure of both the compounds are compared. It is observed that the lowest valence band in Figure 12 and Figure 13 ranging from -12 eV to -9eV in both the spins is almost entirely due to the Z (Si/Ge) s electrons. It is separated from the other hybridized bands because this part of the valence band is not affected by the strong hybridization of Co-Mn atoms. The upper dispersed bands in the valence band are due to the strong hybridization of the Mn-Co 3d electrons. The dispersed bands in the conduction region of minority spin are due to both Mn and Co d electrons [11].

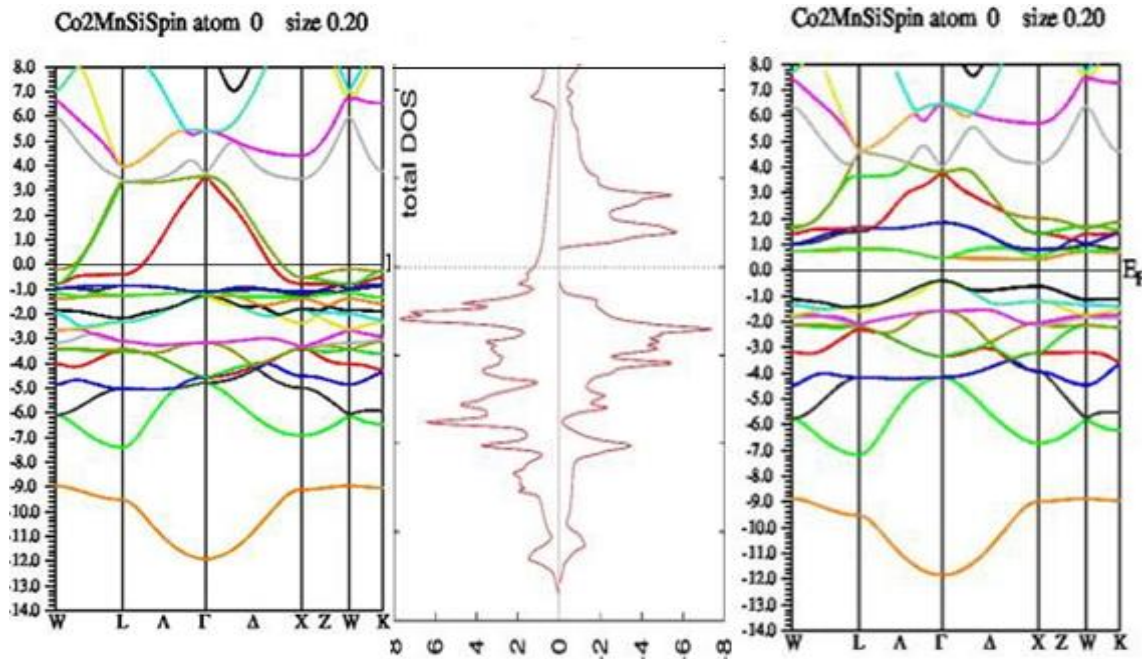


Figure 12: Band structure and TDOS of Co₂MnSi

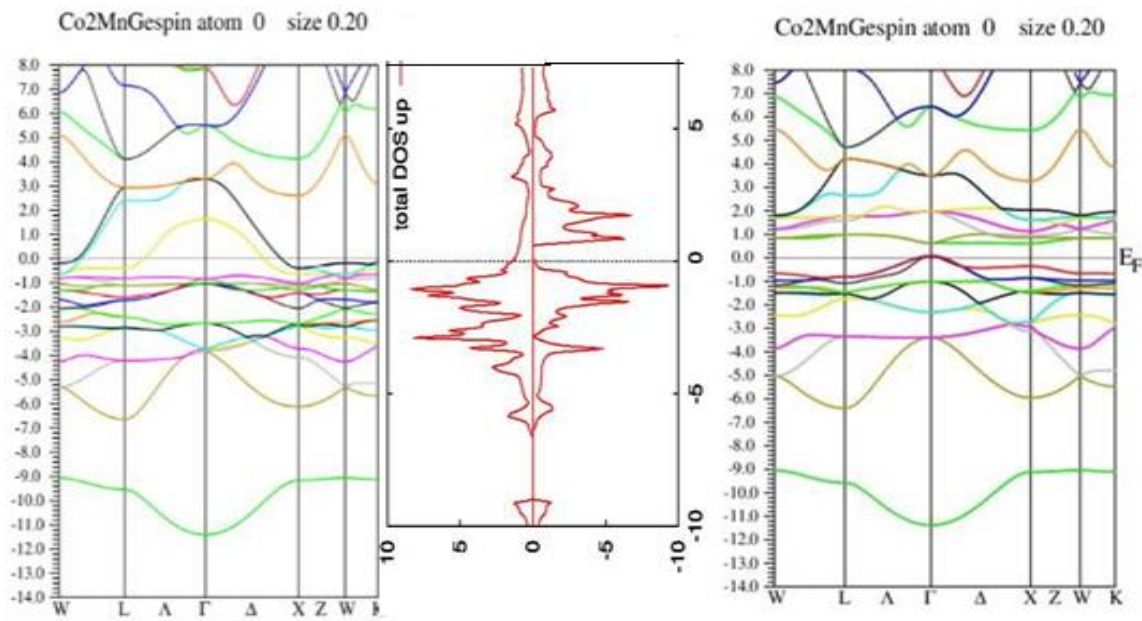


Figure 13: Band structure and TDOS of Co₂MnGe

3.2 Optical Properties

The optical properties of a material are of great interest because it denotes the different ways in which light of different energies can interact with matter. In this work various optical parameters like real and imaginary dielectric constant, electron energy loss, refractive index and extinction coefficient, absorption and optical conductivity are studied using Wien2k application by FPLAPW method in PBE-GGA potential [12].

3.2.1 Dielectric constant

The dielectric constant is the most basic optical properties with which other properties can be

calculated. Dielectric constant consists of real and imaginary parts. The real part is related to the stored energy within the medium and the imaginary part to the dissipation of energy within the medium [13]. The dielectric function gives the linear response of the material to the electromagnetic radiation. The complex dielectric function $\epsilon(\omega)$ is expressed as follows.

$$\epsilon(\omega) = \epsilon_1(\omega) + i\epsilon_2(\omega) \dots\dots\dots 1)$$

Where $\epsilon_1(\omega)$ is the real part of the dielectric function and $\epsilon_2(\omega)$ is the imaginary part of the dielectric function [5]. From $\epsilon(\omega)$ other optical properties can be calculated using Kramers-Kronig relation[3]. The real and imaginary parts of the dielectric constants for the

compounds Co_2MnSi and Co_2MnGe are in Figure 14 (a)(b) and Figure 15(a)(b). From Figure 14(a) and Figure 15(a) the static dielectric constant for the real part is given as 53.002 and 62.0065 for Co_2MnSi and Co_2MnGe respectively. Similarly, the static dielectric constant from Figure 14(b) and Figure 15(b) for the imaginary part is 6.2 and 10.2 for Co_2MnSi and Co_2MnGe respectively. Using these other optical

parameters are analyzed. The dielectric function of the material determines how the material responds to the electromagnetic fields. The static dielectric constant screens the electric fields inside the material generated by trapped charge density [14]. The static dielectric constant is the dielectric constant related to the material behavior in low frequencies or constant electric fields.

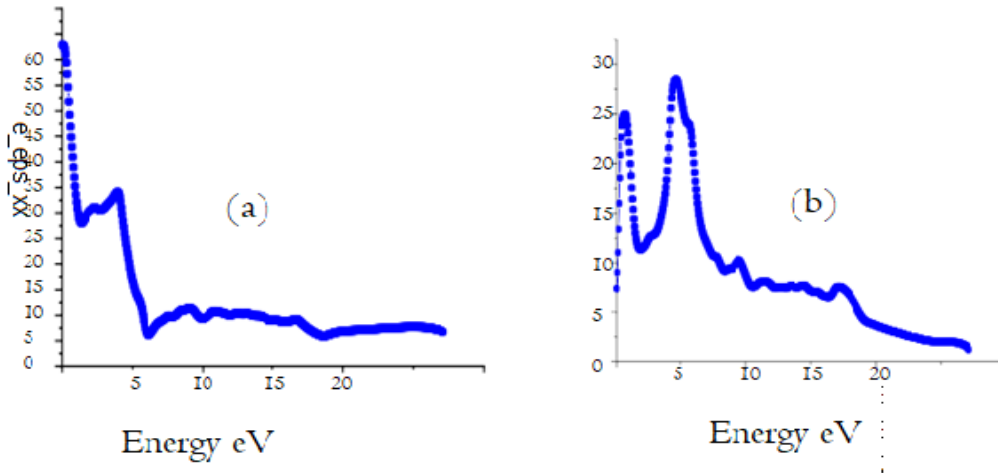


Figure 14: Co_2MnSi - a) Real part of dielectric function $\epsilon_1(\omega)$ b) Imaginary part of dielectric function $\epsilon_2(\omega)$

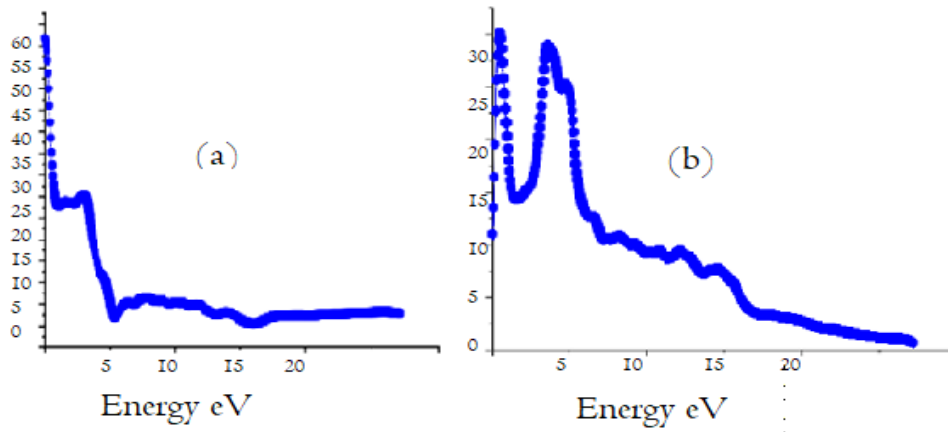


Figure 15: Co_2MnGe - a) Real part of dielectric function $\epsilon_1(\omega)$ b) Imaginary part of dielectric function $\epsilon_2(\omega)$

3.2.2 Absorption coefficient

Absorption coefficient is related to transition between occupied and unoccupied bands due to light and electron interaction [12, 13]. It also indicates the ability of the material to absorb the incident photon of specific energy. It is one of the most important evaluation criteria to identify if the material is optically active or optoelectronic material. The calculated absorption coefficient spectra $\alpha(\omega)$ for the compounds Co_2MnSi and Co_2MnGe is given in Figure 16 (a & b). The absorption graphs in Figure 16 (a&b) starts to increase from 0eV this indicates that both the

compounds start the absorption at very low energy levels. Due to the metallic character of the compounds in the majority spin it may be seen that the absorption begins from a very low incident photon energy [14]. In the visible light spectrum that is around 2eV to 3eV the absorption curve increases rapidly. In the region around 3eV to 4eV the absorption curve decreases and in the energy range of 6eV to 9eV that is in the UV region the curve starts to ascend again. After the energy range of 10eV to 12eV the curve attains a saturation and beyond 12eV the curve starts to ascend indicating the absorption of photon energy by electrons.

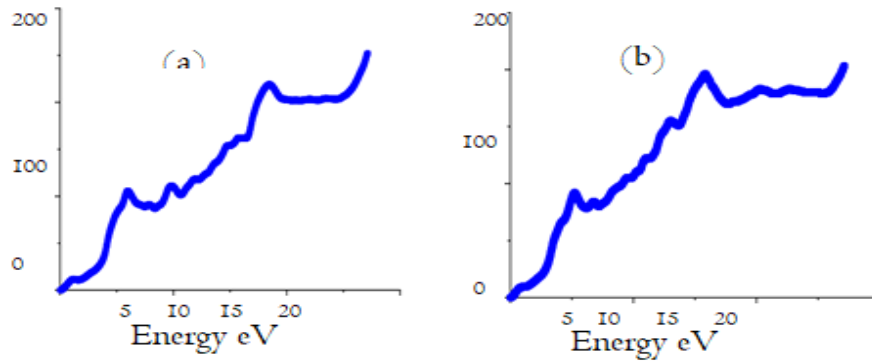


Figure 16: (a) Absorption coefficient of Co_2MnSi , (b) Absorption coefficient of Co_2MnGe

3.2.3 Optical conductivity

The optical conductivity curve reveals that the absorbed light spent to increase the conductivity of the compound [15]. The optical conductivity graphs for the compounds Co_2MnSi and Co_2MnGe is given in Figure 17 and Figure 18. In Figure 17 it could be observed that the conductivity of the material increases as the photon energy increases till 3eV that is the conductivity of the material ascends in the visible region hence this material is suitable for solar cells. Then in the UV limit the conductivity graph decreases till 4 eV beyond this the curve again ascends indicating the increase in conductivity. The maximum conductivity of approximately $9000 \text{ ohm}^{-1}\text{cm}^{-1}$ is observed for 2.2eV energy that is in the visible region. Now considering the optical conductivity for Co_2MnGe compound (Figure 18). The graph is similar to the graph obtained by Co_2MnSi except for the maximum peak values. Co_2MnGe also has high conductivity in the visible region the conductivity is given by $8222.25 \text{ ohm}^{-1}\text{cm}^{-1}$ for the energy range 2.46538 eV.

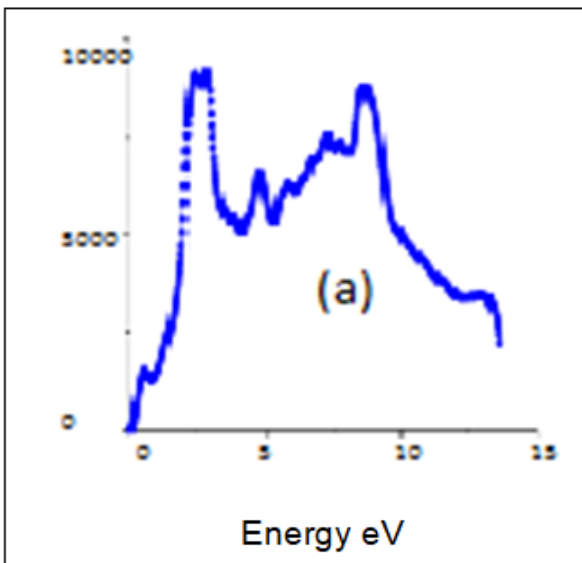


Figure 17: Optical conductivity of Co_2MnSi

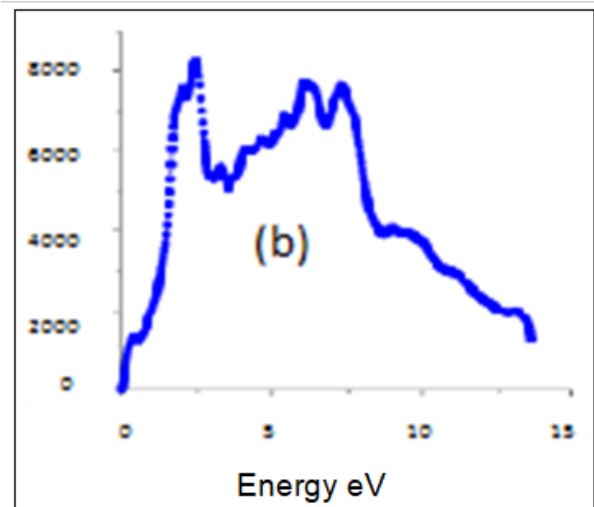


Figure 18: Optical conductivity of Co_2MnGe

3.2.4 Reflectivity and Eloss

Reflectivity and reflection coefficient $R(\omega)$ is a measure of the amount of electromagnetic radiation reflected from the incident medium. Reflectivity determines the opacity of the material calculated from $\epsilon_1(\omega)$ and $\epsilon_2(\omega)$ [16]. The reflectivity graph for Co_2MnSi and Co_2MnGe are given in Figure 19 and Figure 20. As the external radiation incident on the material, some of the valence electrons may undergo inelastic scattering leading to loss of energy. The electron energy loss is given in Figure 21 and Figure 22 for Co_2MnSi and Co_2MnGe . The loss of energy is denoted by $L(\omega)$. The $L(\omega)$ is minimum at lower energies and gradually increases as the photon energy increases. Similarly, the reflectivity is also low for lower energies for both the compounds. For Co_2MnSi as the photon energy increases that are beyond 1.8eV the reflectivity also increases. The static reflectivity for Co_2MnSi is 0.58 and Co_2MnGe is 0.6. It attains a maximum value at 3.2eV, the $R(\omega)$ is around 0.56 beyond 3.5eV the curve starts to descend. In the energy range of 4eV to 9eV the reflectivity or the reflection coefficient remains low indicating the transparency of the material in this energy range. As mentioned earlier this energy range comes under the ultraviolet spectrum thus the material is transparent for the ultraviolet range. When reflectivity for Co_2MnGe is considered (Figure

20), the graph looks similar to Co₂MnSi except for the maximum peak points. The maximum value is 0.57 for 2.5eV beyond which the graph descends. The reflection is very low in the energy range of 3.8eV to 5.8eV which is in the ultraviolet region. Beyond 6eV the graph tends to ascend showing an increase in reflectivity [17].

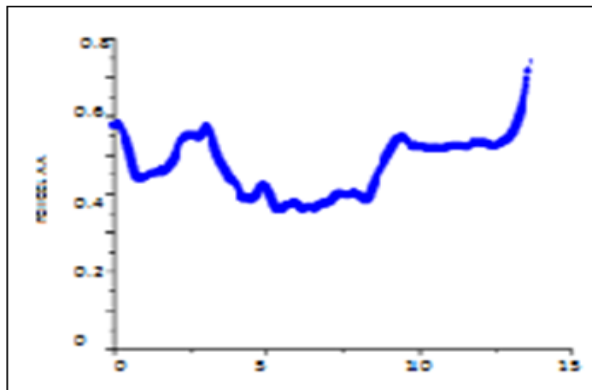


Figure 19: Reflectivity of Co₂MnSi

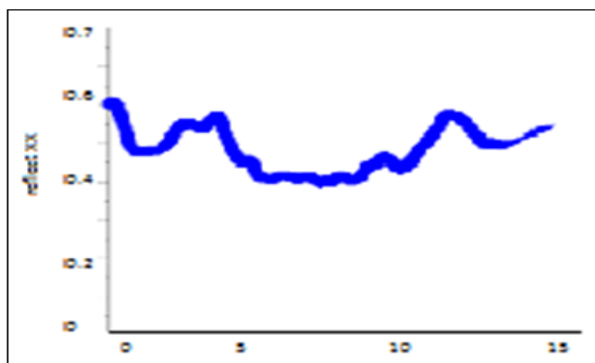


Figure 20: Reflectivity of Co₂MnGe

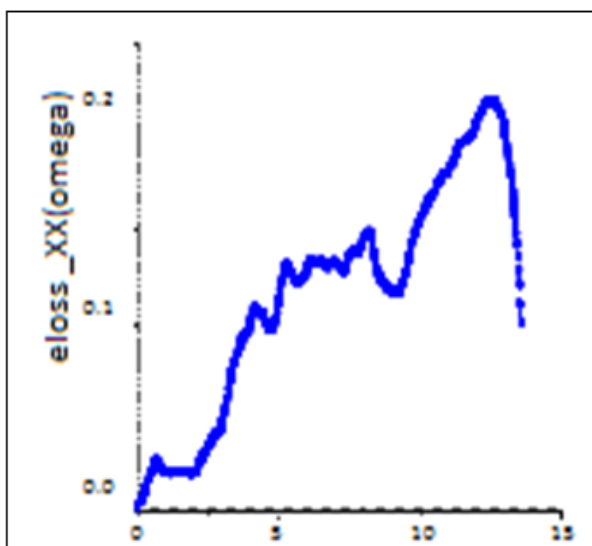


Figure 21: Eloss of Co₂MnSi

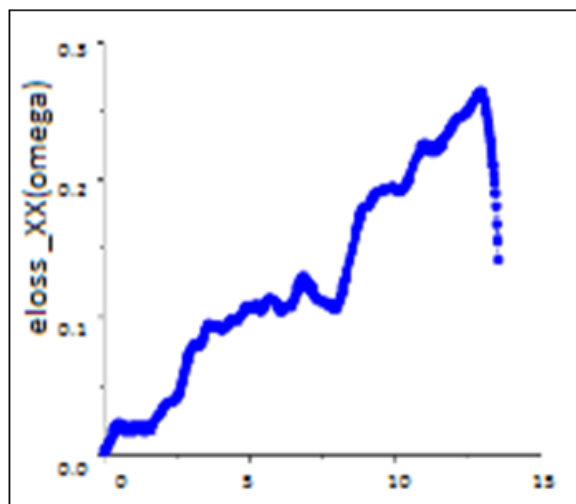


Figure 22: Eloss of Co₂MnGe

3.2.4 Refractive Index and Extinction Coefficient

Refractivity is a very important optical parameter derived from the complex dielectric function. The real part of refractivity is refractive index $n(\omega)$ and the imaginary part is $k(\omega)$ extinction coefficient [17].

The Refractive index is a dimensionless quantity that determines how much light is bent or refracted when entering into a material [13]. The idea of the refractive index of an optical material is important because of its significant use as optical tools such as waveguides, photonic crystals, etc.,. The refractive index signifies the phase velocity and the extinction coefficient signifies the amount of absorption energy loss of the electromagnetic waves when propagates throughout the material. The refractive index and extinction coefficient for Co₂MnSi and Co₂MnGe is given in Figure [23-26]. From Figure 23 and 24 the static refractive index and extinction coefficient of Co₂MnSi is given by 7.3 and 0.5.

Similarly, for Co₂MnGe the static refractive index and extinction coefficient is given as 7.92812 and 0.7 respectively. The static refractive index and $\epsilon_1(0)$ is related as [18];

$$n(0)^2 \sim \epsilon_1(0) \dots\dots\dots (45)$$

That is the square of the static refractive index is approximately equal to static real dielectric constant.

Table 4

Compound	$n(0)$	$n(0)^2$	$\epsilon_1(0)$
Co ₂ MnSi	7.3	53.29	53.002
Co ₂ MnGe	7.92812	62.8551	62.0065

Thus, Table 4 agrees with the above relation. From Figures 24 and 26 it is observed that the refractive index is higher or active for lower energies and as the photon energy increases the refractive index decreases [19]. Whereas the extinction coefficient for both compounds (Figure 24 and Figure 26) is low at 0eV and

increases as the energy increases. The maximum peak is around 3.5eV and 2.5eV for Co_2MnSi and Co_2MnGe respectively then the graph descends. The peaks in the refractive index arise due to interband transitions between the topmost valence band and the lowermost conduction band.

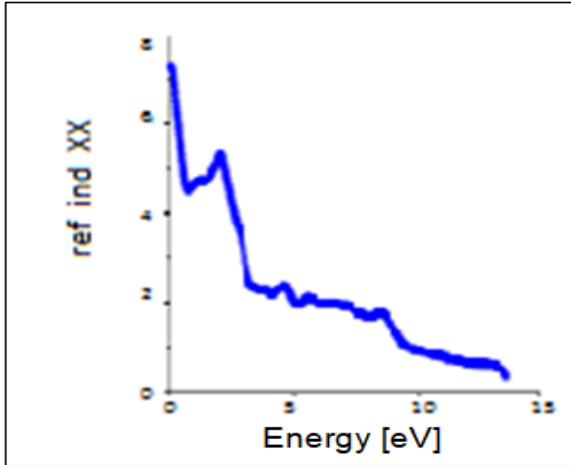


Figure 23: Refractive Index of Co_2MnSi

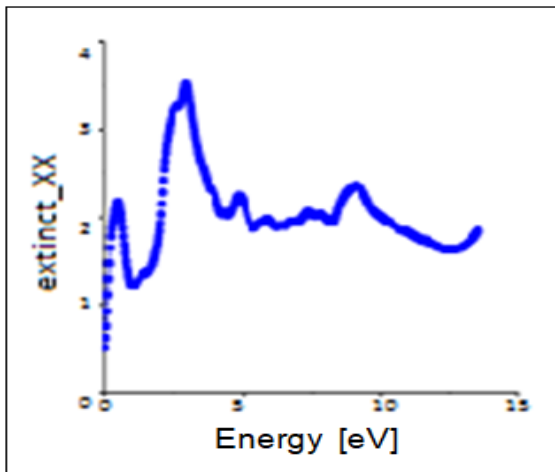


Figure 24: Extinction Coefficient of Co_2MnSi

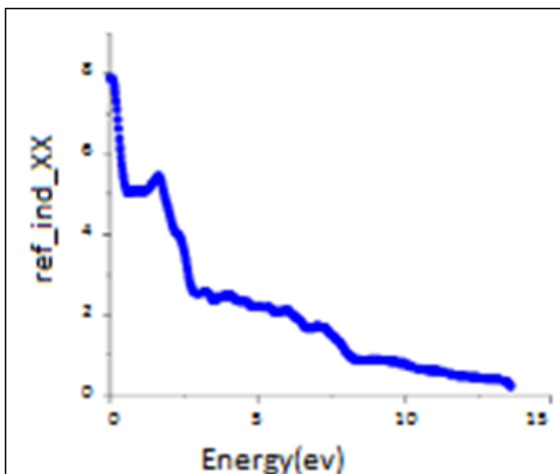


Figure 25: Refractive Index of Co_2MnGe

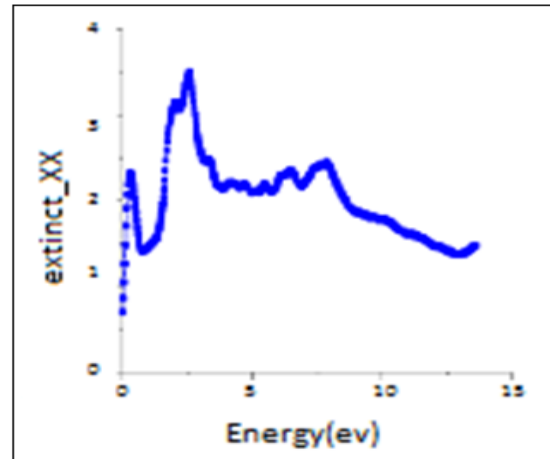


Figure 26: Extinction Coefficient of Co_2MnGe

4. CONCLUSION

To conclude the structural, electronic and optical properties of Co_2MnZ ($Z = \text{Si, Ge}$) as full Heusler compound were computed through FP-LAPW method using WIEN2K code. Exchange correlation effect were included using PBE-GGA potential in the framework of spin polarized DFT. The ground state properties of Co_2MnZ ($Z = \text{Si, Ge}$) is obtained using Birch-Murnaghan's equation of state. The equilibrium parameters such as volume, energy of ground state, bulk modulus and pressure derivative of bulk modulus are derived. These data show that the compound Co_2MnSi is more stable than Co_2MnGe . Furthermore, the stability is proved by the bond length analysis, where the bond length for Co_2MnSi is small than Co_2MnGe . Our results show that the lattice constant increases, volume increases and the bulk modulus decreases by changing the anion atomic number from Si to Ge. The electron density and contour map for the compounds are analyzed using the equilibrium lattice constant. The contour map for Co_2MnSi and Co_2MnGe shows that the covalency is more in minority spin than majority spin. The Density of states and the band structure for the compounds are obtained and observed that in both DOS and band structure half-metallicity is observed in both the compounds. The compounds are of great importance in the field of spintronics due to its halfmetallicity. The band structures are compared with the total DOS to analyze the contribution of electrons in the valence and conduction bands. In minority spin eg-t_{2g} hybridization is observed and it is the reason for the origin of the band gap resulting in half metallic behavior. Thus, both the compounds have metallic nature in the majority spin and semiconducting nature in minority spin. The optical properties for Co_2MnSi and Co_2MnGe are analyzed using the dielectric function. Properties like absorption, refractive index, reflection, eloss and optical conductivity are studied for both the compounds. It is important to note that the optical conductivity for both the compounds is large in the visible region thus making it suitable material for the application as solar cell. The peaks in the imaginary part of dielectric are commonly resulted from interband transitions. The

peaks observed in the absorption coefficient have corresponding dips in the reflectivity for the same energy range. The static dielectric constant and static refractive index relation is related by the relation $n(0)^2 \sim \epsilon_1(0)$ and this relation holds good for the values obtained from the graph and the values are tabulated in table 4. The peaks in the refractive index arises due to interband transitions between the top most valence band and lower most conduction band.

Thus, the studied structural, electronic and optical properties for Co_2MnZ ($Z = \text{Si, Ge}$) shows that the compounds are perfect candidates for various spintronics applications and have extensive research interest in recent years. Studying the magnetic and thermoelectric properties of these compounds would possibly be the future scope of this work. Understanding these properties about Heusler compounds would pave way for further applications in various fields.

REFERENCES

- Perdew, J. P., Burke, K., & Ernzerhof, M. (1996). Generalized gradient approximation made simple. *Physical review letters*, 77(18), 3865.
- Blaha, P., Schwarz, K., Madsen, G. K. H., Kvasnicka, D., & Luitz, J. (2006). WIEN2K, An Augmented Plane Wave, Local Orbitals Program for Calculating Crystal Properties (Tech. Univ. Wien, Austria, 2001); C. Ambrosch-Draxl and J. O. Sofo, *Comput. Phys. Commun.* 175, 1.
- Bainsla, L., & Suresh, K. G. (2016). Equiatomic quaternary Heusler alloys: A material perspective for spintronic applications. *Applied Physics Reviews*, 3(3), 031101.
- Galanakis, I. (2015). High spin-polarization in ultrathin $\text{Co}_2\text{MnSi}/\text{CoPd}$ multilayers. *Journal of Magnetism and Magnetic Materials*, 377, 291–294. doi:10.1016/j.jmmm.2014.10.030
- Yu, G. H., Xu, Y. L., Liu, Z. H., Qiu, H. M., Zhu, Z. Y., Huang, X. P., & Pan, L. Q. (2015). Recent progress in Heusler-type magnetic shape memory alloys. *Rare Metals*, 34(8), 527-539.
- Graf, T., Felser, C., & Parkin, S. S. P. (2011). Simple rules for the understanding of Heusler compounds. *Progress in Solid State Chemistry*, 39(1), 1–50. doi: 10.1016/j.progsolidstchem.2011.02.001
- Lantri, T., Bentata, S., Bouadjemi, B., Benstaali, W., Bouhafs, B., Abbad, A., & Zitouni, A. (2016). Effect of Coulomb interactions and Hartree-Fock exchange on structural, elastic, optoelectronic and magnetic properties of Co_2MnSi Heusler: A comparative study. *Journal of Magnetism and Magnetic Materials*, 419, 74–83. doi:10.1016/j.jmmm.2016.06.01
- Galanakis, I., & H. Dederichs, P. (2006). Half-Metallicity and Slater-Pauling Behavior in the Ferromagnetic Heusler Alloys. *Lecture Notes in Physics*, 1-39. doi:10.1007/11506256_1
- Candan, A., Uğur, G., Charifi, Z., Baaziz, H., & Ellialtıođlu, M. R. (2013). Electronic structure and vibrational properties in cobalt-based full- Heusler compounds: A first principle study of Co_2MnX ($X = \text{Si, Ge, Al, Ga}$). *Journal of Alloys and Compounds*, 560, 215–222. doi:10.1016/j.jallcom.2013.01.102
- Abid, O. M., Menouer, S., Yakoubi, A., Khachai, H., Omran, S. B., Murtaza, G., ... Verma, K. D. (2016). Structural, electronic, elastic, thermoelectric and thermodynamic properties of the NbMSb half heusler ($M = \text{Fe, Ru, Os}$) compounds with first principle calculations. *Superlattices and Microstructures*, 93, 171–185. doi:10.1016/j.spmi.2016.01.001
- Abraham, J. A., Pagare, G., & Sanyal, S. P. (2015). Electronic Structure, Electronic Charge Density, and Optical Properties Analysis of GdX_3 ($X = \text{In, Sn, Tl, and Pb}$) Compounds: DFT Calculations. *Indian Journal of Materials Science*, 1-11. doi:10.1155/2015/296095
- Kandpal, H. C., Fecher, G. H., & Felser, C. (2007). Calculated electronic and magnetic properties of the half-metallic, transition metal based Heusler compounds. *Journal of Physics D: Applied Physics*, 40(6), 1507-1523.
- Bennacer, H., Berrah, S., Boukourt, A., & Ziane, M. I. (2015). Electronic and optical properties of GaInX 2 ($X = \text{As, P}$) from first principles study.
- Lashgari, H., Abolhassani, M. R., Boochani, A., Sartipi, E., Taghavi-Mendi, R., & Ghaderi, A. (2016). Ab initio study of electronic, magnetic, elastic and optical properties of full Heusler Co_2MnSb . *Indian Journal of Physics*, 90(8), 909-916.
- Peng, B., Zhang, H., Shao, H., Xu, Y., Zhang, R., & Zhu, H. (2016). The electronic, optical, and thermodynamic properties of borophene from first-principles calculations. *Journal of Materials Chemistry C*, 4(16), 3592-3598.
- Van der Heide, P. A. M., Baelde, W., De Groot, R. A., De Vroomen, A. R., Van Engen, P. G., & Buschow, K. H. J. (1985). Optical properties of some half-metallic ferromagnets. *Journal of Physics F: Metal Physics*, 15(3), L75.
- Picozzi, S., Continenza, A., & Freeman, A. J. (2002). Co_2MnX ($X = \text{Si, Ge, Sn}$) Heusler compounds: An ab initio study of their structural, electronic, and magnetic properties at zero and elevated pressure. *Physical Review B*, 66(9), 094421.
- BALCI, G., & AYHAN, S. (2019). The first principle study: structural, electronic and optical properties of X_2ZnN_2 ($X: \text{Ca, Ba, Sr}$). *Journal of Non-Oxide Glasses Vol*, 11(1), 9-18.
- Mehmood, N., Ahmad, R., & Murtaza, G. (2017). Ab initio investigations of structural, elastic, mechanical, electronic, magnetic, and optical properties of half-Heusler compounds RhCrZ ($Z = \text{Si, Ge}$). *Journal of Superconductivity and Novel Magnetism*, 30(9), 2481-2488.